

LAUDE: LLM-Assisted Unit Test Generation and Debugging of Hardware DEsigns

Deeksha Nandal^{1*}, Riccardo Revalor¹, Soham Dan^{2†}, Debjit Pal^{1*}

¹Dept. of Electrical and Computer Engineering,
University of Illinois Chicago, Chicago IL 60607,

²Microsoft,

Correspondence: dpal2@uic.edu

Abstract

Unit tests are critical in the hardware design lifecycle to ensure that component design modules are functionally correct and conform to the specification before they are integrated at the system level. Thus developing unit tests targeting various design features requires deep understanding of the design functionality and creativity. When one or more unit tests expose a design failure, the debugging engineer needs to diagnose, localize, and debug the failure to ensure design correctness, which is often a painstaking and intense process. In this work, we introduce LAUDE, a unified unit-test generation and debugging framework for hardware designs that cross-pollinates the semantic understanding of the design source code with the Chain-of-Thought (CoT) reasoning capabilities of foundational Large-Language Models (LLMs). LAUDE integrates prompt engineering and design execution information to enhance its unit test generation accuracy and code debuggability. We apply LAUDE with closed and open-source LLMs to a large corpus of buggy hardware design codes derived from the VerilogEval dataset, where generated unit tests detected bugs in up to 100% and 93% of combinational and sequential designs and debugged up to 93% and 84% of combinational and sequential designs, respectively.

1 Introduction

As hardware systems become ubiquitous and more complex, the verification of functional correctness of such systems is becoming the biggest bottleneck (Veira et al., 2018). Debugging functional bugs in hardware designs written in hardware description languages (HDLs) is an iterative time-consuming process. Verification engineers identify design bugs and refine the designs using a test-based environment where a set of valid inputs is

*Equal contribution by DN and RR.

†SD and DP jointly supervised this work.

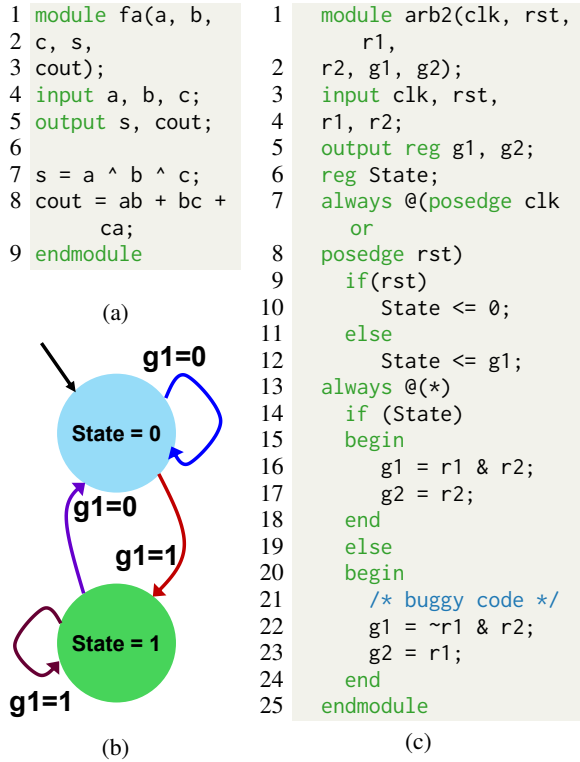


Figure 1: (a) A 1-bit full adder. (b) An FSM capturing correct behavior of a 2-port arbiter. (c) A buggy arbiter. provided to the designs and reasoned over failures to address the root cause. Such inputs are called unit tests and often require a deep understanding of design architecture and functionality. Unlike software, HDLs behavior unfolds over clock cycles and depends on registers, finite-state machines (FSMs), and concurrent logic. As a result, creating unit tests that reliably expose functional errors requires significant manual effort and experience.

Consider 1-bit full adder (FA) of Figure 1a, the FSM of a 2-port arbiter (Arb) of Figure 1b, and a buggy Arb of Figure 1c. For FA, outputs (s, cout) depend only on inputs (a, b, c), much like a software function. However, for the Arb, the outputs (g1, g2) depends on inputs (r1, r2, g1, g2), State, clock (clk), and an asynchronous reset (rst). Lines 22 – 23 contain the bug that causes

Arb to diverge from the desired behavior of the FSM. However, that buggy code will be executed only when `State = 0`. One would require a unit test to drive the Arb to `State = 0` to sensitize the bug, requiring creativity and deep understanding of the Arb behavior captured by the FSM.

Recent research has explored using LLMs for various hardware design and verification tasks to improve syntactic correctness and functional coherence. It remains underexplored whether LLMs can reason and generate test inputs that can trigger and propagate the bugs to observable outputs. This is challenging since it requires reasoning across clock cycles, interactions in FSMs, and is heavily dependent on an implementation (c.f., Figure 1). Additionally, a unit test, upon failure, should produce a trace that is sufficiently divergent and contain a distinct failure signature for successful debugging. However, there is an acute lack of research that explores the reasoning abilities of LLMs to debug design by developing unit tests.

In this work, we propose LAUDE that cross-pollinates semantic understanding of design code, advanced reasoning such as CoT, prompt engineering, and simulation feedback to address the challenges for unit test generation and source code debugging for hardware designs. To evaluate LAUDE, we use a buggy dataset derived from VerilogEval (Liu et al., 2023) containing 1,560 buggy codes (10 buggy codes for each of the 156 problems) by randomly injecting one representative bug from a set of commonly occurring bug types. Our experiments show that unit tests detected bugs in up to 100% and 93% of combinational and sequential designs and debugged up to 93% and 84% of combinational and sequential designs, respectively, thereby establishing effectiveness of LAUDE.

2 Background and Preliminaries

Notations. We consider SystemVerilog (SV) as the primary HDL; however, our technique can be extended to other HDLs, *e.g.*, Verilog, VHDL, etc. We consider a hardware design \mathcal{D} in SV as an SV program for source code analysis. Let \mathcal{V} be the set of design variables, $\mathcal{I} \subset \mathcal{V}$ be the set of input variables, and $\mathcal{O} \subset \mathcal{V}$ be the set of output variables. A unit test \mathcal{U} for a design \mathcal{D} is defined as the binary value ($\mathbb{B} \in [0, 1]$) assignment to all input variables over \mathcal{N} clock cycles, *i.e.*, $\mathcal{I} \mapsto \mathbb{B}^{m \times \mathcal{N}}$ where $|\mathcal{I}| = m$. A **simulation run** with respect to (w.r.t) \mathcal{U} is a time-stamped \mathcal{N} cycle sequence of

design variables $v \in \mathcal{V}$ values from input to output. A **simulation trace** \mathcal{T} w.r.t \mathcal{U} is the set of all simulation runs for all inputs going to outputs. A simulation run is a **failure run** w.r.t a variable $v \in \mathcal{O}$ if $\exists n \in \mathcal{N}$ such that $v^n \neq v_{expected}^n$ (*i.e.*, a value mismatch) where $v_{expected}^n$ is the expected value of variable v at cycle n and $v^n \in \mathcal{T}_f$ (failure trace). We annotate such a design code as a buggy code \mathcal{D}_B . A simulation run is a **passing run** if $\forall v \in \mathcal{O}$, $\forall n \in \mathcal{N}$, $v^n == v_{expected}^n$ (*i.e.*, value match) and produces a passing trace \mathcal{T}_p . We annotate such a design code as the correct code \mathcal{D}_C . We assume an oracle \mathbb{O} (*e.g.*, a functional model of design \mathcal{D}) that can simulate the correct design behavior. This is a reasonable assumption since such models are usually developed during conceptualization.

VerilogEval Dataset. VerilogEval is a hardware design benchmarking suite targeted toward evaluating LLM’s performance in the context of hardware design and verification (Liu et al., 2023). VerilogEval consists of 156 design problems from a Verilog instructional website (HDLBits, 2025) segregated into a set of 82 combinational designs and 74 sequential designs with complex finite state machines (FSMs). Each design problem consists of a reference SV code implementation and a reference testbench to simulate the correct design behavior.

3 LAUDE Methodology

Problem Statement. Given a natural language description \mathcal{L} of a hardware design \mathcal{D} and an oracle \mathbb{O} , we generate a unit test \mathcal{U} such that when \mathcal{U} applied to \mathcal{D} , it produces an output that is consistent with \mathbb{O} ’s output on \mathcal{U} (*i.e.*, \mathcal{T}_p). Our problem has the following assumptions – (i) we consider a *parameterized unit test* $\mathcal{U}(i_1, i_2, \dots, i_m)$ where we treat each design input $i_k \in \mathcal{I}$ as a parameter and assign a set of binary values to each input, and (ii) we establish *functional correctness* of the design by simulating it with a set of $\mathcal{U}(i_1, i_2, \dots, i_m)$ and ensuring the output matches the expected output. For brevity, we will denote $\mathcal{U}(i_1, i_2, \dots, i_m)$ as \mathcal{U} .

3.1 Unit Test Generation Technique

We consider a unit test \mathcal{U} to be valid for design \mathcal{D} if $\mathcal{D}_C(\mathcal{U}) \sim \mathcal{T}_p$. We plan to develop a unit test generator \mathbf{G}_Θ with hyperparameters Θ to generate a valid unit test \mathcal{U} such that $\mathbf{G}_\Theta(\mathcal{L}) \mapsto \mathcal{U}$ without any designer intervention. However, given that a hardware design has a specific set of inputs and output signals (*e.g.*, request, data, acknowledge, etc.)

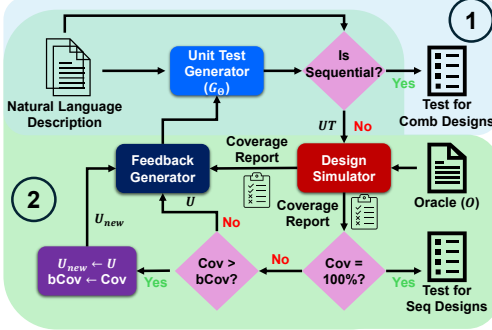


Figure 2: **Iterative unit test generation of LAUDE.** G_E : Generator of Section 3.1. Cov: Coverage information. $bCov$: Best coverage until current iteration. U : Unit test. **Feedback Generator**: Combines coverage information and the unit test for the next iteration.

many of which can be of multibits (*e.g.*, a data bus of width 8 bits), it is important that we provide the design input/output description (*signature*) \mathcal{S}_D as an input to the generator $G_E(\mathcal{L}, \mathcal{S}_D)$. Such signatures can be easily obtained from the design source code via lightweight source code parsing (Mike Popoloski, 2024). Since the key usage of a unit test is to establish the functional correctness of a specific HDL implementation of a hardware design, we include the (potentially) buggy implementation \mathcal{D}_B in the generator input $G_E(\mathcal{L}, \mathcal{S}_D, \mathcal{D}_B)$. The intuition here is that by exposing the generator G_E to \mathcal{D}_B , it can semantically analyze the source code and identify a set of binary input values that will produce a failure trace exposing the deviation from the design intent as expressed in the description \mathcal{L} , *i.e.*, $\mathcal{D}_B(U) \sim \mathcal{T}_f$. We use various closed and open source foundational LLMs for G_E (c.f., Section 4). A key objective of the unit test generation technique is that the unit test should produce a significant divergent trace \mathcal{T}_f compared to the output of the \mathbb{O} when applied to the buggy code \mathcal{D}_B . **In our analysis**, we evaluate and compare $G_E(\mathcal{L}, \mathcal{S}_D)$ (NLS) and $G_E(\mathcal{L}, \mathcal{S}_D, \mathcal{D}_B)$ (NLSC) as generator techniques. Our initial experiments showed that NL often generates unit tests that are syntactically and/or semantically incorrect and cannot be simulated. In future work, we will further investigate NL and will compare it with NLS and NLSC.

Figure 2 shows the iterative unit test generation flow which uses a structured prompt as shown in Figure 3 to incorporate necessary information (*i.e.*, $\mathcal{L}, \mathcal{S}_D, \mathcal{D}_B$) for unit test generation. For combinational circuits (shown in blue with ①), the U generation is a one-shot process. For sequential circuit, its iterative (shown in green with

```

1 You are a Verilog test case generator [specializing in sequential circuits]. Your task is to generate <NUM_TESTS> unit tests that [can expose bugs | are diverse] for this module:
2
3 Module: <MODULE_NAME>
4 Input ports: <INPUT_LIST>
5 Output ports: <OUTPUT_LIST>
6 Verilog code: <VERILOG_CODE>
7 Task: <TASK_DESCRIPTION>
8 [Requirements:]
9 [- Focus on sequential circuits and expose bugs.
  ]
10 [- Use key=value pairs matching port order.]
11 [- Use Verilog notation (e.g., 1'b0).]
12 Output format (one per line):
13 { "task_id": <ID>, "inputs": "<ASSIGNMENTS>" }
14 Generate <NUM_TESTS> [bug-exposing | diverse] unit tests:

```

Figure 3: **Example prompt to guide an LLM (G_E) for unit test generation.** The prompt specifies task description (\mathcal{L}), module signature (\mathcal{S}_D), likely buggy design code (\mathcal{D}_B), and formatting requirements, encouraging the generation of diverse, bug-exposing unit tests while preserving port ordering and design notation.

②). The G_E aims to generate an unit test that has significant design coverage (w.r.t oracle \mathbb{O}), *e.g.*, FSM coverage, and accepts a newly generated unit test only when the coverage increases. We provide the coverage report to G_E to aid its generation process.

3.2 Unit Test-Assisted Debugging Technique

A concern for using the automatically generated unit test U with debugging is that the unit tests can be noisy, *i.e.*, they could be inaccurate with two serious implications – (i) the unit test U fails to *sensitize* the bug in the likely buggy design code \mathcal{D}_B creating a passing trace \mathcal{T}_p due to U 's failure to execute design paths containing the bug in \mathcal{D}_B , thereby pointing to the *insufficient coverage of the design source code* and (ii) the unit test may have activated the bug, however, its effect got *masked* before propagating to an output to create a \mathcal{T}_f , thereby indicating the generator's *insufficient semantic understanding of the design source code*. Both these types of errors are **detrimental** to debugging, as they could potentially remove the likely buggy code \mathcal{D}_B from the debugging process early on, without actually fixing the bug. To tackle these problems, we propose an *iterative* debugging approach of Figure 4.

We begin with the potentially buggy code

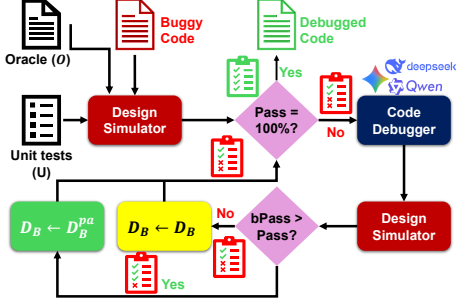


Figure 4: **Unit-test driven iterative debugging of LAUDE.** D_B : Buggy code. D_B^{pa} : Patched code after debugging with LLM. **Pass**: Fraction of unit tests passed. **bPass**: Best Pass until current iteration.

D_B , a unit test that has generated a failing trace \mathcal{T}_f , and a summary of the mismatches that are symptomatic of the failure. Intuitively, the mismatches provide the failure signature that needs to be investigated to localize the buggy code. We use a structured prompt as shown in Figure 5 to incorporate the necessary information for the LLM and ask it to generate a likely debugged code D_B^{pa} . However, the D_B^{pa} may introduce additional bugs (since LLMs are probabilistic models) or may not fix the original bug at all. Hence, instead of accepting the patched code immediately, we rerun all the unit tests on D_B^{pa} and only accept the D_B^{pa} if it increases the fraction of unit tests that produce passing trace \mathcal{T}_p . The iteration continues until all unit tests pass or a fixed number of iterations is completed (we set it to 5).

4 Experimental Setup

Dataset. We develop a new dataset from VerilogEval for evaluating LAUDE. We have created a database of commonly occurring functional bug types (*e.g.*, logical bugs, improper/missing state transitions) from open-sourced hardware design code repositories. We have used Gemini-2.5 Pro to mutate the reference design code of each problem included in VerilogEval by injecting a representative bug of the respective bug type at a time, and create ten different buggy design codes (BC01, BC02, ..., BC10) for each problem, totaling to a total of 1,560 (156×10) buggy codes.

LLMs Used. We have used multiple open-source and closed-source reasoning and coding LLMs to evaluate the effectiveness of LAUDE. Table 1 details the LLMs that we

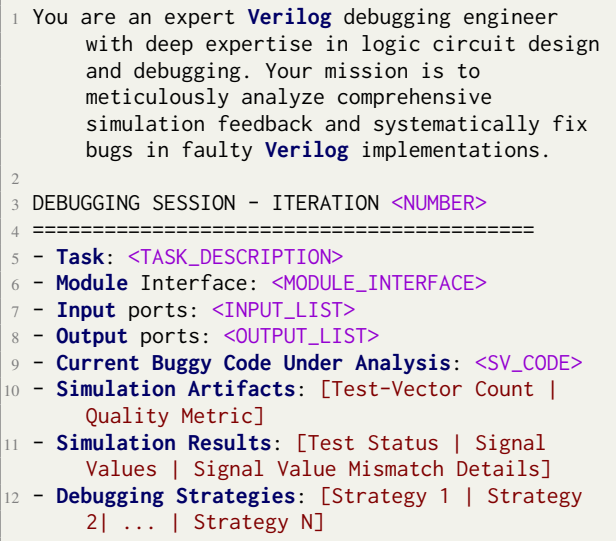


Figure 5: **Example prompt to guide an LLM for debugging.** The prompt specifies the task description (\mathcal{L}), likely buggy design source code (D_B), and formatting requirements, encouraging the generation of corrected code while preserving port ordering and design notation. **Debugging Strategies** include *Clock Domain Analysis*, *Reset Logic Verification*, *State Machine Analysis*, *Edge Detection*, *Data Path Synchronization* among others.

Table 1: **Details of the LLMs used in the experiment.**

LLM Name	LLM Type	# of LLM Parameters
Gemini-2.5 Pro	Closed Source	Not disclosed
DeepSeek R1-Distill-Qwen	Open Source	32B
Gemini-2.5 Flash	Closed Source	Not disclosed
Qwen-2.5 Coder-Instruct	Open Source	32B

have used. DeepSeek-R1-Distill-Qwen-32B ([DeepSeek-AI, 2025](#)) is fine-tuned from the Qwen-2.5-32B ([Qwen et al., 2025](#)) base model using a dataset generated by the DeepSeek-R1 (671B) model. We selected this model to *test if advanced reasoning capabilities are effective for hardware design and validation tasks* in a locally deployable fashion. We included Qwen-2.5 Coder-32B-Instruct ([Hui et al., 2024](#)) to *test how a model specialized for code generation would perform against more generalist models*. For DeepSeek and Qwen we used the original FP16 precisions, and vLLM ([Kwon et al., 2023](#)) as the inference engine. We show the results for Gemini-2.5 Flash and Qwen-32B in Section B.

Hardware Platform Used. We used (i) two (2) NVIDIA RTX 6000 Ada GPUs, leveraging tensor parallelism ([Narayanan et al., 2021](#)) and (ii) a NVIDIA H200 GPU, leveraging its massive high-bandwidth memory (HBM3e) to maximize the execution speed.

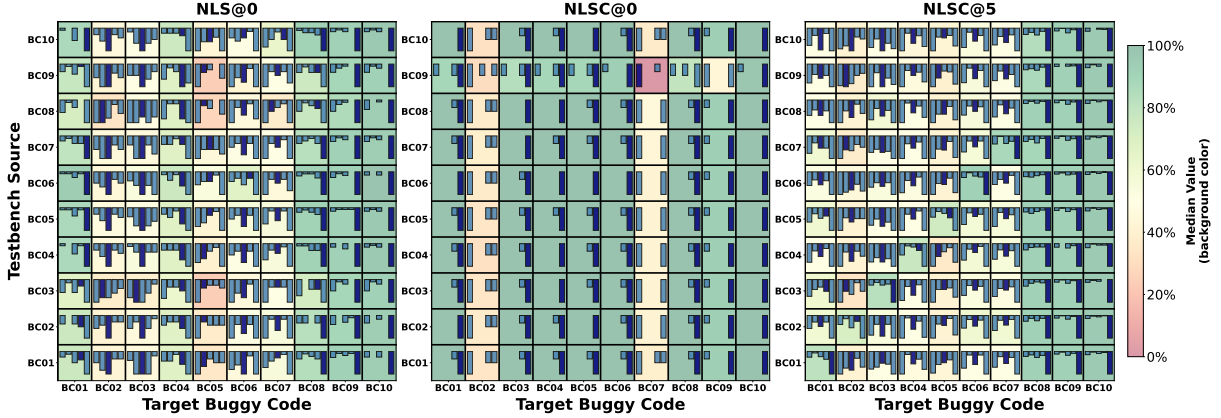


Figure 6: **Divergence Rate (DR)** distribution for Gemini-2.5 Pro. The 10×10 box glyph heatmap with sparklines utilize equally spaced 5-bin scale: **Bin 1 (0%–20%)** through **Bin 5 (80%–100%)** from left to right. The darkest bar in the sparkline indicates the bin containing the median value, which also determines the cell’s background color. NLS@0 shows weakest performance. NLSC@0 and NLSC@5 achieve the best results, primarily concentrated at **Bin 5 (80%–100%)** regardless of the testbench source.

Hyperparameters. For all test generator and debugging techniques, we maintained consistent hyperparameters (Θ) to ensure fair comparison – *temperature* set to 0.8 to *balance creativity with determinism*. The *output token generation limits* were set based on the deployment infrastructure. For open-source models, we used a dual strategy to optimize the throughput, consisting of 2,048 for NLSC (to accommodate code-specific reasoning), and 512 for NLS and NL. For closed-source models, we used the API’s maximum token limit, delegating resource management to the provider’s infrastructure. We restricted the *input context window* to 16,384 tokens for all open-source models. Although, this number is well below the model’s theoretical maximum taken, we found it to be sufficient to contain the largest design and testbench codes in our datasets with reasonable Key-Value (KV) cache memory footprint with efficient execution without Out-of-Memory errors. We set the *maximum GPU memory* utilization to 0.95 for vLLM. The remaining 0.05 of VRAM memory acts as a swap space for temporary tensors and KV pairs.

Metrics. We measure the effectiveness of LAUDE by quantifying the *sensitivity* (**Attack Rate (AR)**) and *specificity* (**Divergence Rate (DR)**) of the unit tests. A unit test is *sensitive* if it can detect many different bugs in a design and creates a \mathcal{T}_f . A unit test is *specific* if it can generate a failure trace \mathcal{T}_f that is divergent as compared to a passing trace \mathcal{T}_p and carries a

unique failure signature for a bug. We use *Divergent Attack* (DA) to quantify the goodness of a unit test w.r.t sensitivity and specificity.

Attack Rate (AR). Attack Rate quantifies the bug detectability of a unit test \mathcal{U} when applied on a \mathcal{D}_B and is computed as the fraction of problems for which a \mathcal{T}_f is produced. The AR for i^{th} problem is computed as $AR_i = 1$ if \mathcal{T}_f , otherwise 0. The overall attack rate is computed as $AR = \frac{\sum_{i=1}^N AR_i}{N}$, where N is the total number of problems. A higher AR indicates the effectiveness of unit tests in bug detection.

Divergence Rate (DR). Divergence Rate quantifies how different/divergent a failure trace \mathcal{T}_f is as compared to a passing trace \mathcal{T}_p when the same unit test \mathcal{U} is applied on a likely buggy design \mathcal{D}_B and an oracle \mathbb{O} , respectively. DR is measured as $DR = \frac{\sum_{i=1}^n |\mathcal{T}_p[i] \neq \mathcal{T}_f[i]|}{n}$, where $|\mathcal{U}| = n$. A higher DR value indicates a significant amount of mismatch between \mathcal{T}_p and \mathcal{T}_f , yielding an informative failing trace for debugging. **Note** while AR measures bug detectability, DR measures bug debuggability.

Divergent Attack (DA). Divergent Attack quantifies the bug detectability and debuggability of a unit test \mathcal{U} in a unified way. Intuitively, a test should be capable of detecting a broad spectrum of bugs (*i.e.*, sensitive to bugs) and generate a unique failure signature for a bug to aid debugging (*i.e.*, specific to the effects of the bug). Consequently, we compute DA as $DA = DR \cap AR$, *i.e.*, a unit test \mathcal{U} will have

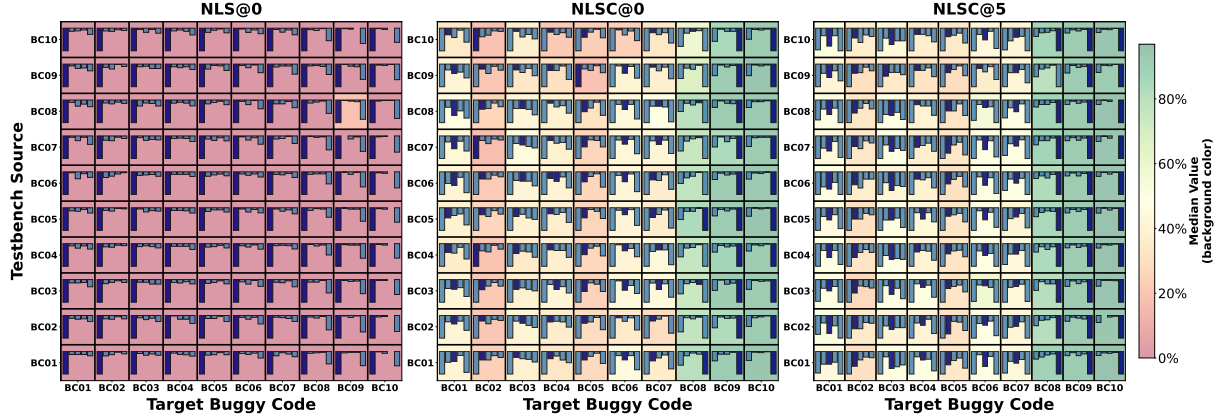


Figure 7: **Divergence Rate (DR) Distribution for DeepSeek R1** using 10×10 box glyph heatmap with 5-bin sparklines as Figure 6. NLS@0 is predominantly concentrated in Bin 1 (0% – 20%). The NLSC@0 shows mixed results with high variance. NLSC@5 demonstrates better performance, particularly on targets BC08 – BC10.

higher DA *if* it has both high AR and DR.

Experimental Categories: We primarily compare 0-shot of NLS (denoted as NLS@0) and 0-shot and 5-shot of NLSC, denoted as NLSC@0 and NLSC@5, respectively.

We have used Synopsys® VCS V-2023.12-1 to simulate SV designs (-sverilog flag) and collect coverage information (-cm flag).

5 Experimental Results

In this Section, we evaluate the goodness of the generated tests for bug detection and debugging using the buggy design benchmark.

5.1 Bug Sensitivity Analysis of Unit Tests

In this experiment, we evaluate *how sensitive the generated unit tests are w.r.t bug detection*. Toward that, for a given hardware design task, we generated unit tests from the i^{th} buggy code, $i \in [1, 10]$ and applied it on BC01, …, BC10. See Section A for the detailed sparkline plots (c.f., Figures 11 and 12).

The results show different behaviors across the two LLMs. For Gemini-2.5 Pro, NLS@0 is highly effective, consistently achieving AR values falling in the fifth bin ($> 80\%$). This performance remains stable in NLSC@0 and NLSC@5, with the exception of NLSC@0, where the AR for Source BC09 against Target BC07 drops significantly to $< 20\%$. DeepSeek R1 is ineffective with NLS@0; AR distributions remain largely in the lowest quartile ($< 20\%$), except for specific targets (BC03 and BC08) which show higher susceptibility.

However, the NLSC@0 and NLSC@5 configurations drastically improve DeepSeek R1’s performance, raising the AR to levels that are competitive with Gemini Pro ($> 80\%$) across all targets. *This experiment demonstrates that contextual grounding is a critical requirement for DeepSeek R1 to overcome generation volatility and achieve competitive bug sensitivity.*

5.2 Bug Specificity Analysis of Unit Tests

In this experiment, we evaluate *the goodness of the unit tests in generating bug-specific failure signature* using the setup of Section 5.1. Figures 6 and 7 show the DR for Gemini-2.5 Pro and DeepSeek R1, respectively.

To visualize the *central tendency* of DR distribution, the color of each cell represents the median DR, mapped to a color scale where **red** and **green** indicate worse (0%) and optimal performance (100%), respectively. To correlate the DR distribution with its central metric, we show the bin containing the median in a darker shade for a simultaneous assessment of variance and the mean efficacy of the unit tests.

For NLS@0, Gemini-2.5 Pro performs the worst characterized by distributions spreading more evenly across intermediate bins. However, Gemini-2.5 Pro demonstrates consistency across the NLSC@0 and NLSC@5, achieving up to 100% (average 90%) DR for BC08 – BC10. However, NLSC@0 shows a specific vulnerability for BC02 and BC07, exhibiting a performance drop. This shows that while buggy code generally aids LLM’s unit test gen-

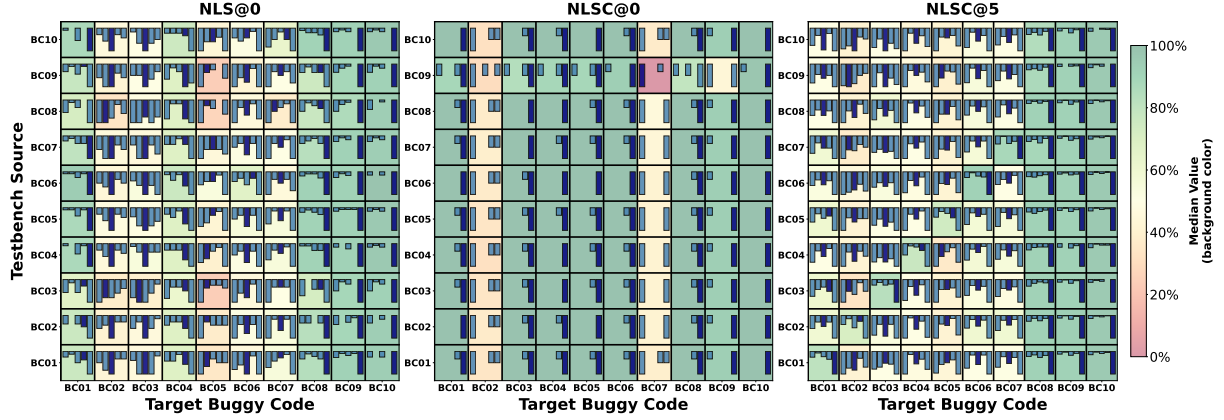


Figure 8: **Divergent Attack (DA) Distribution for Gemini-2.5 Pro** using 10×10 box glyph heatmap with 5-bin sparklines. NLSC@0 and NLSC@5 achieve the highest results, especially for BC08 – BC10. For BC01 – BC07, we observe higher variance, as DA falls into multiple distinct bins.

eration, specific bug types may act as adversarial examples, degrading the model’s ability to generate unit tests for divergent failure trace.

DeepSeek R1 shows a *high sensitivity* to the unit test generation strategy. The NLS@0 is concentrated in Bin 1 (0% – 20%), indicating a near-total inability to generate divergent traces without context. The NLSC@0 shows high variance, struggling to achieve the high-performance of Gemini-2.5. The NLSC@5 shows an improved ability to generate divergent traces, particularly for BC08 – BC10. ***This experiment shows that the DeepSeek R1 heavily rely on few-shot examples to reason and achieve competitive performance.***

5.3 Debuggability Analysis of Unit Tests

In this experiment, we quantify *the goodness of a unit test for bug detection and generating a divergent failure trace*. Figures 8 and 9 show the DA for Gemini-2.5 Pro and DeepSeek R1.

For Gemini-2.5 Pro, the DA distributions closely mirror the distributions observed in Section 5.2. Both NLSC@0 and NLSC@5 achieve high DA values within 80% – 100% for BC08 – BC10. However, for BC01 – BC07, DA drops to intermediate bins despite non-zero AR, revealing cases where bugs are detected but insufficiently propagated through the design to produce sustained divergence. This shows that successful attacks do not guarantee *strongly divergent failure traces*. For NL, DeepSeek R1 remains ineffective while NLSC@0 improves performance but suffers from high variance, suggesting un-

stable reasoning when only buggy code is provided. In contrast, NLSC@5 consistently produces high DA scores for complex bug targets, demonstrating that few-shot guidance enables the model to detect bugs and propagate their effects through multiple simulation cycles. ***This experiment shows that generating a unit test for real-world debugging requires creativity that can be challenging for state-of-the-art LLMs.***

5.4 Effectiveness of Iterative Debugging

In this experiment, we evaluate *effectiveness of LAUDE’s iterative debugging process by leveraging the generated unit tests, failure trace \mathcal{T}_f , and simulation feedback*. Figures 10a and 10b show the debugging success rate for combinational and sequential designs, respectively.

For NLS@0, Gemini-2.5 Pro exhibit high success rates (median ≈ 0.85 for combinational and ≈ 0.73 for sequential). In contrast, DeepSeek R1 remains highly unstable; its distribution is notably wide and dispersed (median ≈ 0.5), indicating a lack of consistent reasoning patterns when the model is forced to debug with unit tests generated via NLS@0. In NLSC@0, Gemini-2.5 Pro and DeepSeek R1 result in higher performance. The availability of the source code acts as a critical grounding mechanism for the open-source models. DeepSeek R1 achieve the largest relative gains, with medians reaching between 0.7 and 0.8. This suggests that while these models lack the intuition to generate high-quality unit tests in NLS@0, their reasoning engines are fully ca-

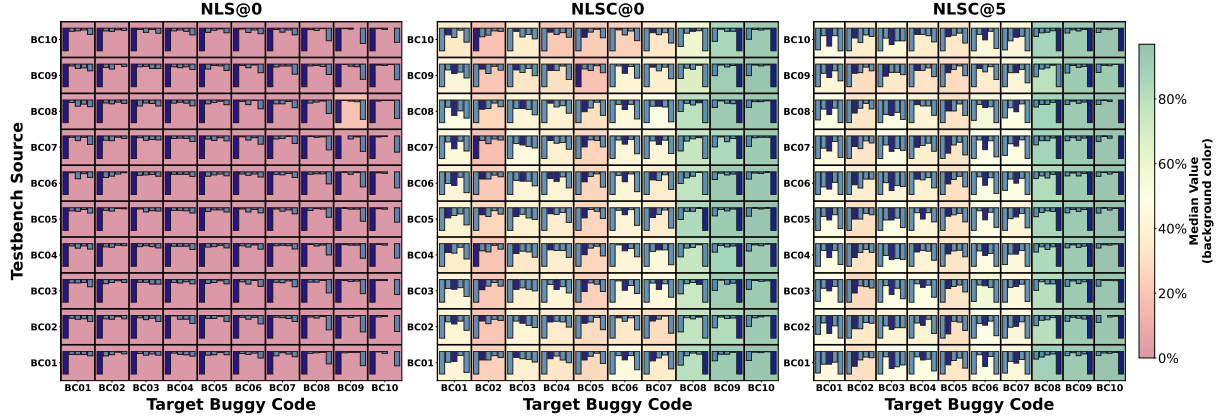


Figure 9: **Divergent Attack (DA) Distribution for DeepSeek R1** using the same format as Figure 8. NLS@0 is predominantly concentrated in Bin 1 (0%–20%) across buggy codes. The NLSC@0 shows mixed results with high variance. NLSC@5 demonstrates the strongest performance, particularly for BC08 – BC10.

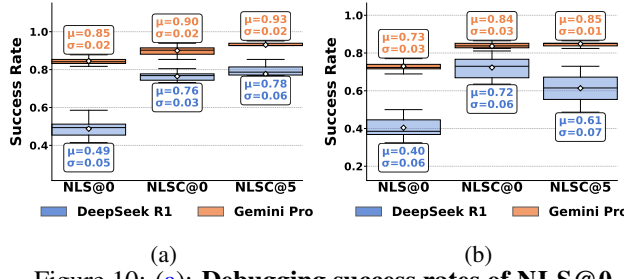


Figure 10: (a): Debugging success rates of NLS@0, NLSC@0, and NLSC@5 for various LLMs for buggy combinational circuit design codes. (b): Debugging success rates of NLS@0, NLSC@0, and NLSC@5 for various LLMs for buggy sequential circuit design codes.

pable of analyzing specific bugs when the design circuit is exposed. The NLSC@5 provides a universal, though more incremental refinement for both LLMs. The NLSC@5 pushes the median success rates for all models above 0.75 for combinatorial, closing the gap between the proprietary and the open-source models. Gemini-2.5 Pro retains a consistent reasoning as evidenced by tighter distributions near the upper bound of the metric compared to the larger variance in the DeepSeek R1.

Overall, the performances of the models across each G_{Θ} are lower for sequential designs than combinational designs. This is attributable to the higher complexity of sequential circuits. ***This experiment shows that while the current LLMs are effective in reasoning for debugging, they struggle to debug buggy designs without additional information.*** See Section C for a more detailed analysis of the density of the results.

6 Related Work

Traditional hardware verification techniques are time-consuming, error-prone, and difficult to scale. Recently, the success of gen-AI, *e.g.*, LLMs, in scientific domains has propelled researchers to leverage LLMs’ reasoning for hardware design and verification tasks.

LLMs for Code Generation. The majority of recent efforts have focused on applying LLMs to *HDL Code Generation* (Zhao et al., 2025; Sun et al., 2025; Vijayaraghavan et al., 2024; Zhang et al., 2024; Chang et al., 2025; Liu et al., 2023; Pinckney et al., 2025; Al Amin et al., 2025). However, these work do not encompass the testing and debugging loops required for robust hardware verification. (Prasad et al., 2025) inspired our work, but does not apply to hardware because of fundamental semantic differences around timing, reasoning across clock cycles, parallelism/concurrency logic, and state machine interactions.

LLM for Hardware Verification. Recent work (Blocklove et al., 2024; Zhang et al., 2025; Qayyum et al., 2024) benchmarked LLMs for hardware design, testbench generation, and hardware verification. However, all these methods require extensive manual prompting and careful integration due to data scarcity and domain complexity. LAUDE leverages LLMs’ reasoning abilities and advanced prompting strategies to fully automate unit test generation and facilitate bug localization.

LAUDE proposes an LLM-assisted **unified framework** for unit test generation and

iterative debugging for hardware designs.

LAUDE’s novelty lies in its closed-loop, coupled, scalable, and iterative methodology. To our knowledge, LAUDE is the first to integrate LLM reasoning with simulation feedback to enhance sensitivity and specificity of unit tests.

7 Conclusion

LAUDE provides a scalable and automated solution for localizing, diagnosing, and debugging functional errors in the hardware design source code using unit tests. The experimental results on a commonly used benchmark and a variety of functional bugs demonstrate its effectiveness in detecting and debugging functional errors. LAUDE demonstrated that while the current closed- and open-source LLMs can reason on complex hardware verification tasks, there are broad scopes for improvement.

8 Limitations

We identify the following limitations of this work in terms of the dataset and the evaluation methodology.

- **Dataset:** In the scope of this study, our primary focus is to establish a fully automated end-to-end unit test generation and debugging methodology using small, controlled, yet representative dataset. Moving forward, it will be interesting to apply this LAUDE to larger datasets. Additionally, LAUDE considers a relatively simple set of circuits each containing a single design module. It would be interesting to increase the complexity of the designs in terms of functionality, module interaction complexity, and code size and evaluate LAUDE on such augmented set of designs.
- **Quantitative Evaluation:** In this work, we primarily focused on unit test generation and debugging without quantifying and ranking the subtleties of the captured design behavior. It would be interesting to include such rankings in the few-shot examples in NL, NLS, and NLSC and evaluate LLM’s capability to automatically rank quality of the debugged code to quantify captured design behavior.
- **Modeling:** In this paper, we assessed the debugging capabilities of state-of-the-art language models. In future work, it will be interesting to fine-tune language models for unit test generation, code generation, debugging, and evaluating their performance using LAUDE. Additionally, it would be interesting to develop language models that can predict design behavior across clock cycles to remove the necessity of the oracle \mathbb{O} in the LAUDE flow.
- **Evaluation:** In future work, it will be valuable to conduct a more detailed evaluation of model errors and robustness to better understand the specific limitations of each LLM for debugging.

References

Rashed Al Amin, Md Golam Rassel Lincoln, and Roman Obermaisser. 2025. Towards LLM-Assisted HDL Generation and Verification. *IEEE Mediterranean Conf. on Embedded Computing (MECO)*.

Jason Blocklove, Siddharth Garg, Ramesh Karri, and Hammond Pearce. 2024. Evaluating LLMs for Hardware Design and Test. *IEEE Int'l Conf. on LLM-Aided Design (LAD)*.

Kaiyan Chang, Ying Wang, Haimeng Ren, Mengdi Wang, Shengwen Liang, Yinhe Han, Huawei Li, and Xiaowei Li. 2025. ChipGPT: How far are we from natural language hardware design. *arXiv*.

Gheorghe Comanici, Eric Bieber, Mike Schaekermann, Ice Pasupat, Noveen Sachdeva, Inderjit Dhillon, Marcel Blistein, Ori Ram, Dan Zhang, Evan Rosen, Luke Marrs, Sam Petulla, Colin Gaffney, Asaf Aharoni, Nathan Lintz, and 1 others. 2025. Gemini 2.5: Pushing the Frontier with Advanced Reasoning, Multimodality, Long Context, and Next Generation Agentic Capabilities. *arXiv preprint arXiv:2507.06261*.

DeepSeek-AI. 2025. DeepSeek-R1-Distill-Qwen-32B. <https://huggingface.co/deepseek-ai/DeepSeek-R1-Distill-Qwen-32B>. Hugging Face model card, MIT License.

HDLBits. 2025. HDLBITS Verilog Language Problems. https://hdlbits.01xz.net/wiki/Problem_sets#Verilog_Language.

Binyuan Hui, Jian Yang, Zeyu Cui, Jiaxi Yang, Dayiheng Liu, Lei Zhang, Tianyu Liu, Jiajun Zhang, Bowen Yu, Kai Dang, and 1 others. 2024. Qwen2. 5-Coder Technical Report. *arXiv preprint arXiv:2409.12186*.

Woosuk Kwon, Zhuohan Li, Siyuan Zhuang, Ying Sheng, Lianmin Zheng, Cody Hao Yu, Joseph E. Gonzalez, Hao Zhang, and Ion Stoica. 2023. Efficient Memory Management for Large Language Model Serving with Paged Attention. *Symp. on Operating Systems Principles (SOSP)*.

Mingjie Liu, Nathaniel Pinckney, Brucek Khailany, and Haoxing Ren. 2023. VerilogEval: Evaluating Large Language Models for Verilog Code Generation. *Int'l Conf. on Computer-Aided Design (ICCAD)*.

Mike Popoloski. 2024. SLANG - SystemVerilog Language Services codecov PyPI . <https://github.com/MikePopoloski/slang>.

Deepak Narayanan, Mohammad Shoeybi, Jared Casper, Patrick LeGresley, Mostofa Patwary, Vijay Korthikanti, Gaurav Venkatesh, Anima Anandkumar, and Bryan Catanzaro. 2021. Efficient Large-Scale Language Model Training on GPU Clusters Using Megatron-LM. *arXiv preprint arXiv:2104.04473*.

Nathaniel Pinckney, Christopher Batten, Mingjie Liu, Haoxing Ren, and Brucek Khailany. 2025. Revisiting VerilogEval: A Year of Improvements in Large-Language Models for Hardware Code Generation. *arXiv preprint arXiv:2408.11053*.

Archiki Prasad, Elias Stengel-Eskin, Justin Chih-Yao Chen, Zaid Khan, and Mohit Bansal. 2025. Learning to Generate Unit Tests for Automated Debugging. *Conf. on Language Modeling (COLM)*.

Khushboo Qayyum, Sallar Ahmadi-Pour, Chandan Kumar Jha, Muhammad Hassan, and Rolf Drechsler. 2024. LLMs for Hardware Verification: Frameworks, Techniques, and Future Directions. *Asian Test Symp. (ATS)*.

Qwen, :, An Yang, Baosong Yang, Beichen Zhang, Binyuan Hui, Bo Zheng, Bowen Yu, Chengyuan Li, Dayiheng Liu, Fei Huang, Haoran Wei, Huan Lin, Jian Yang, Jianhong Tu, Jianwei Zhang, Jianxin Yang, Jiaxi Yang, Jingren Zhou, and 25 others. 2025. *Qwen2.5 Technical Report*. Preprint, arXiv:2412.15115.

Wenhao Sun, Bing Li, Grace Li Zhang, Xunzhao Yin, Cheng Zhuo, and Ulf Schlichtmann. 2025. Paradigm-Based Automatic HDL Code Generation Using LLMs. *arXiv* 2501.12702.

Neil Veira, Zisis Poulos, and Andreas Veneris. 2018. Suspect Set Prediction in RTL Bug Hunting. *Design, Automation, and Test in Europe (DATE)*.

Prashanth Vijayaraghavan, Apoorva Nitsure, Charles Mackin, Luyao Shi, Stefano Ambrogio, Arvind Haran, Viresh Paruthi, Ali Elzein, Dan Coops, David Beymer, Tyler Baldwin, and Ehsan Degan. 2024. Chain-of-Descriptions: Improving Code LLMs for VHDL Code Generation and Summarization. *ACM/IEEE Workshop on Machine Learning for CAD (MLCAD)*.

Yongan Zhang, Zhongzhi Yu, Yonggan Fu, Cheng Wan, and Yingyan Celine Lin. 2024. MG-Verilog: Multi-grained Dataset Towards Enhanced LLM-assisted Verilog Generation. *Int'l Conf. on Computer-Aided Design (ICCAD)*.

Zixi Zhang, Balint Szekely, Pedro Gimenes, Greg Chadwick, Hugo McNally, Jianyi Cheng, Robert Mullins, and Yiren Zhao. 2025. LLM4DV: Using Large Language Models for Hardware Test Stimuli Generation. *arXiv*.

Yang Zhao, Di Huang, Chongxiao Li, Pengwei Jin, Muxin Song, Yinan Xu, Ziyuan Nan, Mingju Gao, Tianyun Ma, Lei Qi, Yansong Pan, Zhenxing Zhang, Rui Zhang, Xishan Zhang, Zidong Du, Qi Guo, and Xing Hu. 2025. CodeV: Empowering LLMs with HDL Generation through Multi-Level Summarization. *arXiv*.

A AR sparkline plots for Gemini-2.5 Pro and DeepSeek R1

Figure 11 shows the AR Sparkline plots for Gemini-2.5 Pro using the NLS@0, NLSC@0, and NLSC@5 configurations, while Figure 12 shows the AR results for DeepSeek R1. These plots corresponds to the AR Sparkline Plot analysis of Section 5.1.

B Experimental Results using Gemini-2.5 Flash and Qwen-2.5 Coder LLMs

In this Section, we evaluate the goodness of the generated tests for bug detection and debugging using the buggy design benchmark, using Gemini-2.5 Flash (Comanici et al., 2025) and Qwen-2.5 Coder (Hui et al., 2024; Qwen et al., 2025) as LLMs.

B.1 Bug Sensitivity Analysis of Unit Tests

In this experiment, we evaluate *how sensitive the generated unit tests are w.r.t bug detection*. Toward that, for a given hardware design task, we generated unit tests from the i^{th} buggy code, $i \in [1, 10]$ and applied it on BC01, ..., BC10. Essentially, the setup is the same as that of Section 5.1.

Figures 13 and 14 show the AR sparkline results. For Qwen, NLS@0 is largely ineffective, with AR distributions consistently stagnating in the lowest quartile ($< 20\%$). However, the transition to NLSC@0 effectively restores performance, shifting the distributions into the $80\% - 100\%$ range for BC08–BC10, a trend that stabilizes further with NLSC@5. In contrast, Gemini-2.5 Flash exhibits exceptional robustness from the outset. Unlike Qwen, it does not suffer from zero-shot collapse; both NLS@0 and NLSC@0 maintain high sensitivity with median ARs consistently $> 90\%$. The NLSC@5 configuration serves only to saturate this already high performance, pushing the AR distributions to $\approx 100\%$. ***This experiment highlights a distinct architectural divergence: while Qwen shows a more gradual capability curve, Gemini-2.5 Flash demonstrates robustness, achieving higher results in all configurations.***

B.2 Bug Specificity Analysis of Unit Tests

In this experiment, we evaluate *the goodness of the unit tests in generating bug-specific failure signature* using the setup of Section B.1. Figures 15 and 16 show the DR for Gemini-2.5 Flash and Qwen-2.5 Coder, respectively.

To visualize the *central tendency* of DR distribution, the color of each cell represents the median DR, mapped to a color scale where **red** and **green** indicate worse (0%) and optimal performance (100%), respectively. To correlate the DR distribution with its central metric, we show the bin containing the median in a darker shade for a simultaneous assessment of variance and the mean efficacy of the unit tests.

For NLS@0, Qwen-2.5 Coder performs the worst characterized by distributions spreading towards the lowest bin (0% - 20%). Gemini-2.5 Flash performs better, achieving the highest results for BC08 – BC10. Moving to the NLSC@0 configuration, Qwen demonstrates a robust architectural recovery, shifting its DR results toward the upper quartiles ($> 50\%$) for almost all bins, proving its capability to utilize instructions to correct its generation logic. In stark contrast, Gemini-2.5 Flash exhibits a concerning rigidity in the NLSC@0 setting; its distributions remain largely static compared to the NLS@0 for the complex targets (BC01—BC07). It is only under the NLSC@5 configuration that both models converge to saturation, but the trajectory differs: Qwen arrives there via steady instruction-following improvements, while Gemini relies entirely on the few-shot context to unlock its high-efficacy states. ***This experiment shows that while Qwen-2.5 Coder progressively improves its reasoning via instruction following, Gemini-2.5 Flash’s detection capability remains latent until unlocked by few-shot examples, exposing Gemini’s critical dependency on in-context learning grounding.***

B.3 Debuggability Analysis of Unit Tests

In this experiment, we quantify *the goodness of a unit test for bug detection and generating a divergent failure trace*. Figures 17 and 18 show the DA for Gemini-2.5 Flash and Qwen-2.5 Coder, respectively.

For Gemini-2.5 Flash, the DA distribu-

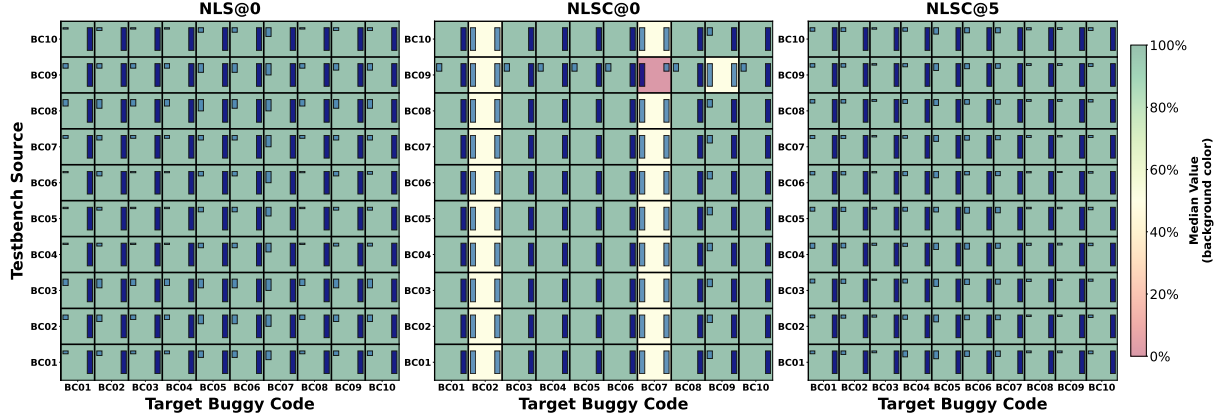


Figure 11: **Attack Rate (AR) Distribution for Gemini-2.5 Pro.** This figure applies the established 10×10 glyph heatmap format with 5-bin sparklines to analyze the performance of Gemini 2.5 Pro. The 10×10 gymph heatmap with sparklines utilize equally spaced 5-bin scale: **Bin 1 (0%–20%)** through **Bin 5 (80%–100%)** from left to right. **Results:** Unlike DeepSeek R1, Gemini-2.5 Pro demonstrates high robustness in the zero-shot NLS@0 setting (dominant green, median $> 80\%$). However, the NLSC@5 configuration introduces unexpected instability, particularly for targets BC02 and BC07 where median AR drops to the 40%–60% range, with a specific collapse ($< 20\%$) for Source BC09 on Target BC07. The few-shot NLSC@5 configuration effectively restores consistent high sensitivity across all pairs.

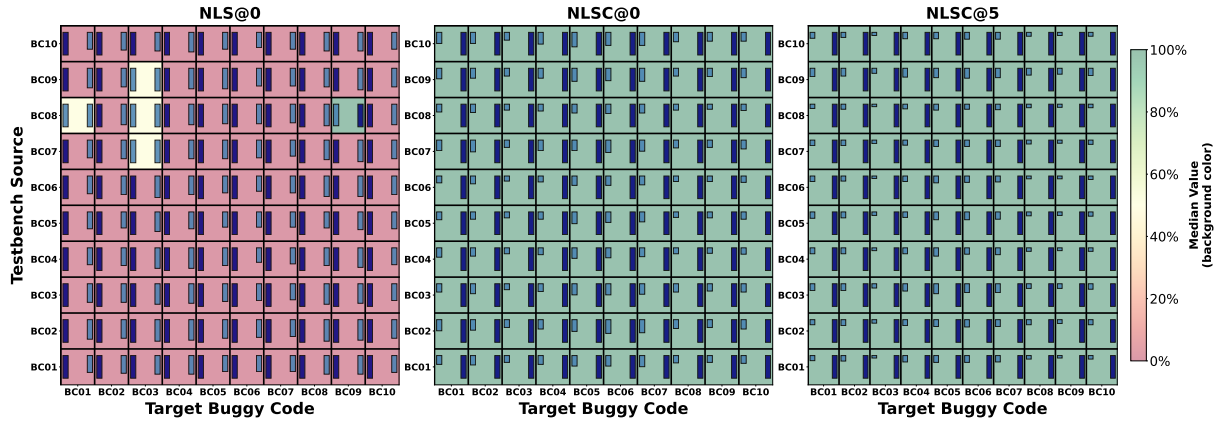


Figure 12: **Attack Rate (AR) Distribution for DeepSeek R1** using the same format as Figure 11. The model largely fails in the zero-shot NL setting (dominant red, median $< 20\%$) but achieves near-universal robustness (dominant green, median $> 80\%$) once structural context is introduced in NLSC@0 and NLSC@5.

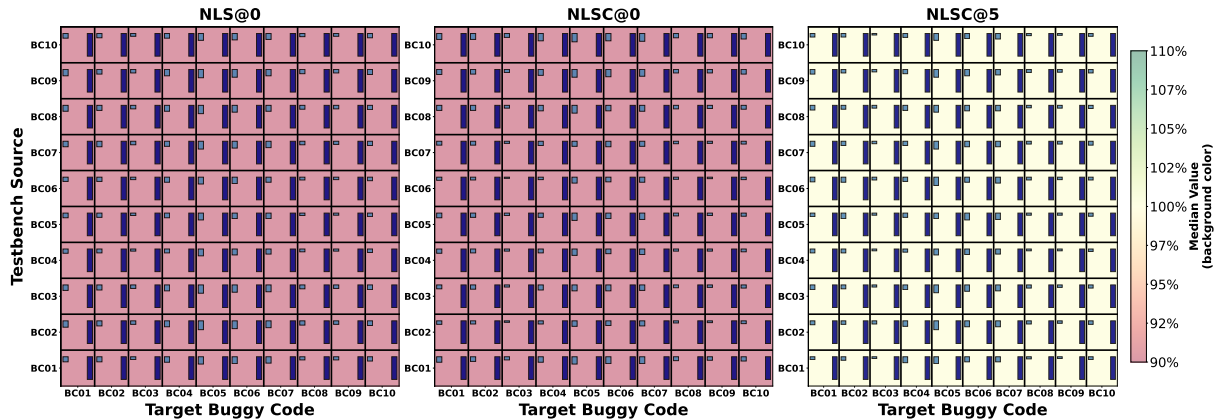


Figure 13: **Attack Rate (AR) Distribution for Gemini Flash.** Gemini-2.5 Flash maintains high sensitivity ($> 90\%$, dominant green) in the NLS@0. The NLSC@0 and NLSC@5 configurations further improve the results, pushing the median AR to $\approx 100\%$ across all targets

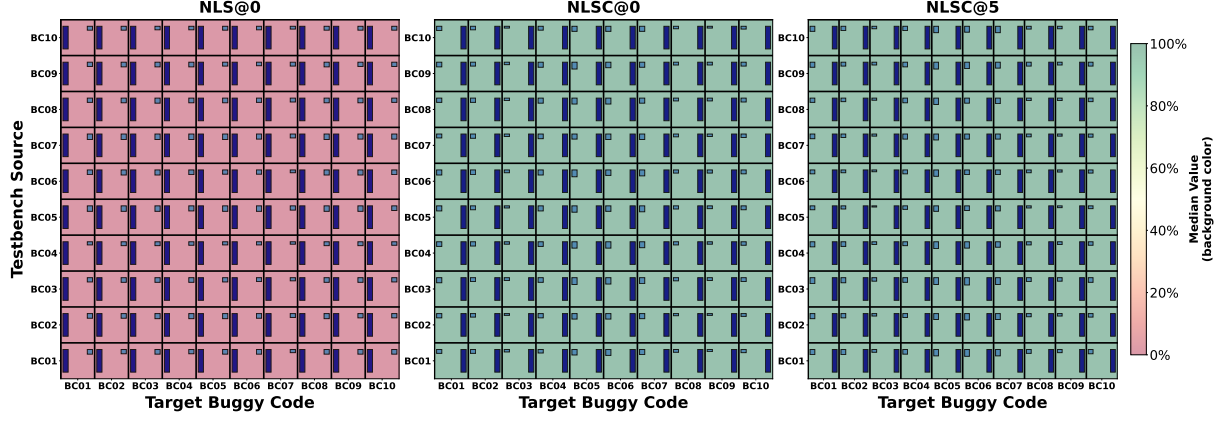


Figure 14: **Attack Rate (AR) Distribution for Qwen-2.5 Coder.** The NLS@0 configuration shows a comprehensive failure (dominant red, median < 20%) across nearly all source-target pairs. However, the introduction of the system prompt in NLSC@0 delivers better AR results, restoring high sensitivity (dominant green, > 80%) for BC08–BC10.

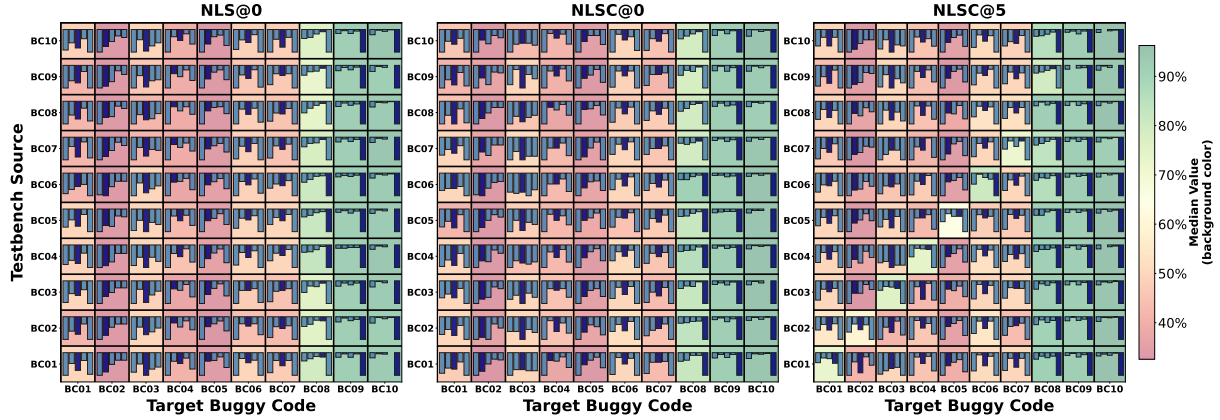


Figure 15: **Divergence Rate (DR) Distribution for Gemini-2.5 Flash.** We observe that Gemini-2.5 Flash exhibits a concerning rigidity in the NLSC@0 setting; its distributions remain largely static compared to the NLS@0 for the complex targets (BC01—BC07).

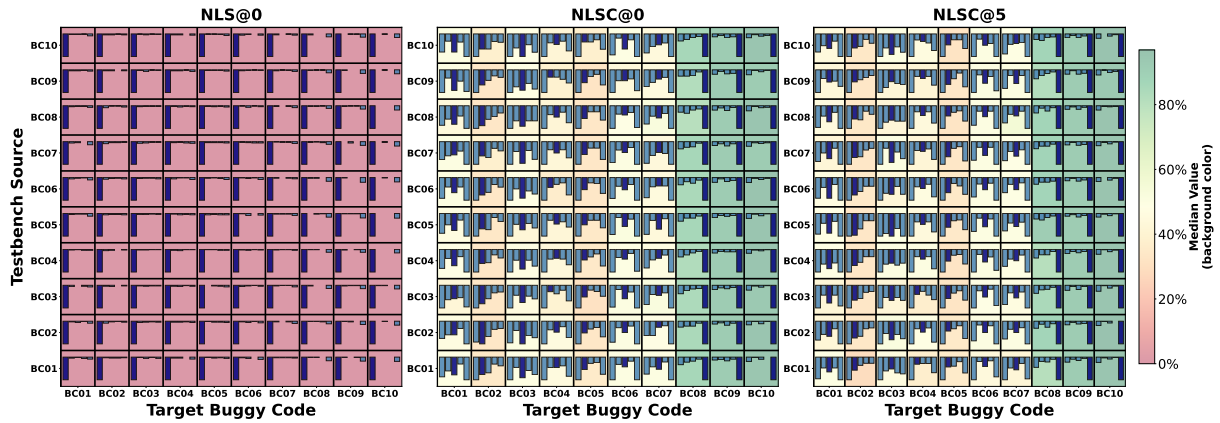


Figure 16: **Divergence Rate (DR) Distribution for Qwen-2.5 Coder.** The sparklines utilize the 5-bin scale: **Bin 1 (0%–20%)** through **Bin 5 (80%–100%)**. *Results:* NLS@0 is predominantly concentrated in Bin 1 (0%–20%) across buggy codes. The NLSC@0 and NLSC@5 demonstrates the strongest performance, particularly for BC08 – BC10.

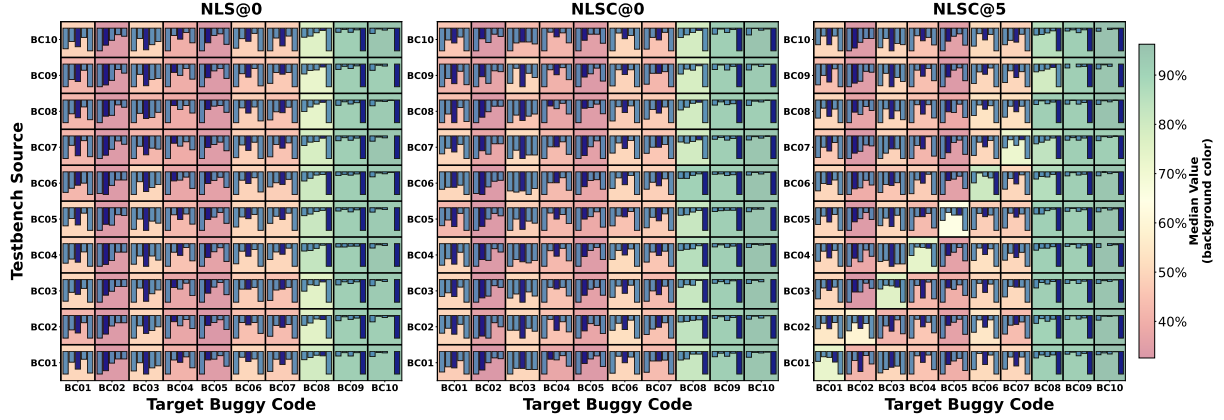


Figure 17: **Divegent Attack (DA) Distribution for Gemini-2.5 Flash.** The observed distributions closely mirror the DR ones, shown in Figure 15. For targets BC01–BC07, performance drops significantly to intermediate levels (Bins 2–3).

tions closely mirror the distributions observed in Section B.2. Specifically, the NLSC@0 configuration fails to yield a substantial improvement over NLS@0, with the majority of targets (particularly BC01 – BC07) remaining trapped in the lower efficacy bins (< 40%). This indicates that simply providing the buggy code is insufficient for the Flash model to achieve satisfactory results, as done by the Pro model. In contrast, Qwen-2.5 Coder demonstrates a decisive shift in the NLSC@0 configuration, where the DA distributions migrate significantly toward the higher bins (60% – 100%). Both models eventually converge to the highest DA results in the NLSC@5 configuration. ***The disparity in the NLSC@0 configuration confirms the results found in the previous analysis in Sections B.1 and B.2***

B.4 Effectiveness of Iterative Debugging

In this experiment, we evaluate the *effectiveness of LAUDE’s iterative debugging process* by leveraging the generated unit tests, failure trace \mathcal{T}_f , and simulation status to repair the faulty code. Figures 19a and 19b show the debugging success rate distribution for combinational and sequential designs, respectively.

The results reveal a striking performance disparity between the models, contradicting the trends observed in testbench generation. For combinatorial circuits, Gemini-2.5 Flash shows high robustness when debugging, maintaining a consistently high mean success rate across all configurations: $\mu = 0.84$ in

NLS@0, $\mu = 0.87$ in NLSC@0, and $\mu = 0.89$ in NLSC@5, which is the most effective configuration. This suggests that for this iterative repair task, Gemini Flash possesses a stable intrinsic debugging capability that is largely independent of the prompt’s context level. On the other hand, Qwen-2.5 Coder shows significant sensitivity and, compared to Gemini Flash, lower performance. In the NLS@0 configuration, it struggles to debug effectively ($\mu = 0.13$), likely due to the lack of context. We can see that providing the faulty code (NLSC@0) yields a substantial improvement to $\mu = 0.72$. Within NLSC@5 configuration, it achieves the best performances overall, but these results are still, on average, 14% lower than what Gemini Flash can achieve. The relative performances of the two LLMs don’t significantly change when focusing on sequential circuits. Due to their inherently higher complexity of sequential, the debugging success rates are lower compared to combinatorial, but Gemini-2.5 Flash still manages to achieve an average success rate $> 80\%$ for any configuration. Qwen performs very poorly on NLS@0, as the distribution is centered towards lower percentages, but manages to gain an average of 44% when shifting to NLSC@0 configuration.

C Debugging Success Rate Distribution Analysis

In this Section, we detail the debugging success rate distributions for the different LLMs we used. To provide a richer understanding of

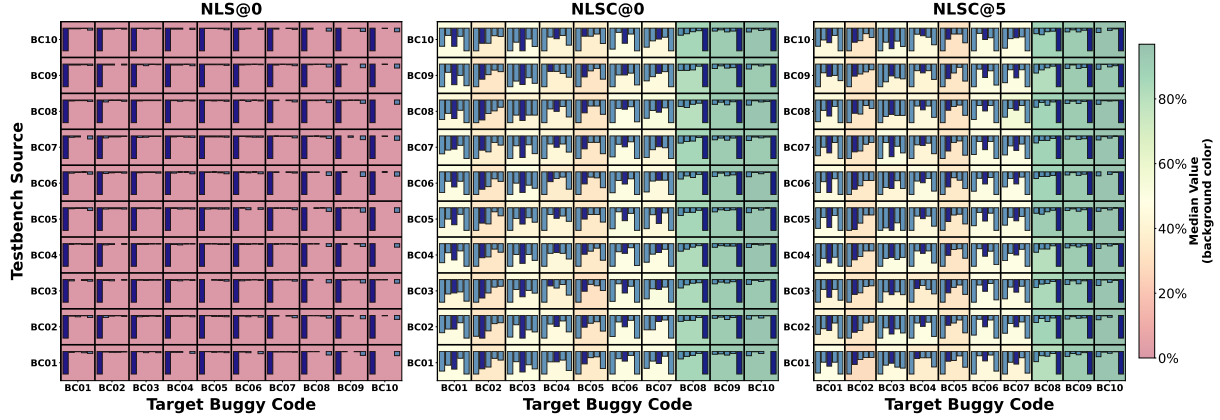


Figure 18: **Divergent Attack (DA) Distribution for Qwen-2.5 Coder.** Qwen demonstrates a pronounced sensitivity to the Target Buggy Code, evidenced by the distinct vertical banding pattern visible across all configurations. Performance is heavily polarized by the target: **BC08–BC10** are consistently solved with high reliability (Green, **Bin 5**), whereas targets like **BC02** and **BC05** remain persistently difficult (lighter columns with scattered distributions) regardless of the method used. The baseline attack Rates are the lowest for all pairs of Target Buggy Code and Testbench source.

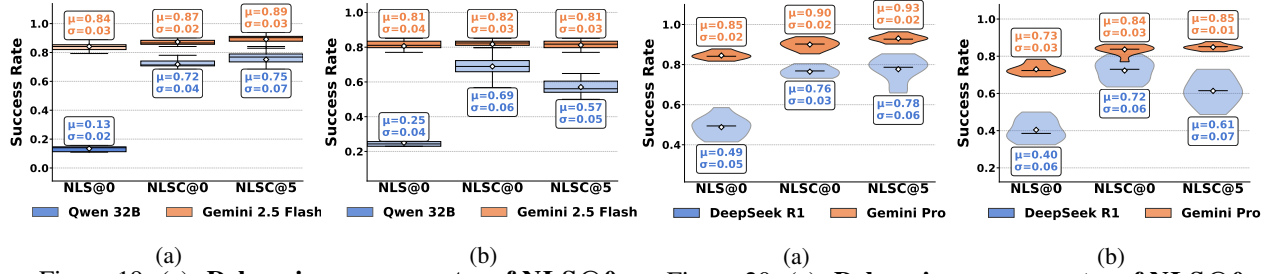


Figure 19: (a): Debugging success rates of NLS@0, NLSC@0, and NLSC@5 for various LLMs for buggy combinational circuit design codes. (b): Debugging success rates of NLS@0, NLSC@0, and NLSC@5 for Gemini-2.5 Flash and Qwen-2.5 32B Coder for buggy sequential circuit design codes.

the model performance distributions beyond simple summary statistics (such as means or medians), we utilize violin plots.

C.1 Interpretation of Violin Plots

The violin plots presented in Figures 20 and 21 combine the features of a box plot with a kernel density estimation (KDE). This visualization technique allows for a comprehensive assessment of the models’ reliability and stability across different prompting strategies. The width of the “violin” at any given y-axis value represents the probability density of the success rate at that level. Wider sections indicate a higher frequency of data points (*i.e.*, the model achieves this success rate more often), while narrower sections indicate rarity. The shape of the plot shows how the data is distributed.

(a)

Figure 20: (a): Debugging success rates of NLS@0, NLSC@0, and NLSC@5 for Gemini-2.5 Pro and DeepSeek R1 for buggy *combinational circuit design codes*. (b): Debugging success rates of NLS@0, NLSC@0, and NLSC@5 for Gemini 2.5 Pro and DeepSeek R1 for buggy *sequential circuit design codes*.

(b)

A bottom-heavy shape means most values are lower, while a top-heavy or wider upper part suggests consistently high performance.

C.2 Effectiveness of Iterative Debugging using Violin Plots

In this Section, we will leverage the interpretation of Section C.1 to provide fine grain insights on the effectiveness of debugging of LAUDE.

C.2.1 Gemini-2.5 Pro and DeepSeek R1

Figure 20a and Figure 20b show the violin plot distributions for the success rates for Gemini-2.5 Pro and DeepSeek R1 across the three configurations. For combinational designs, we can see that for **Gemini-2.5 Pro**, the violin

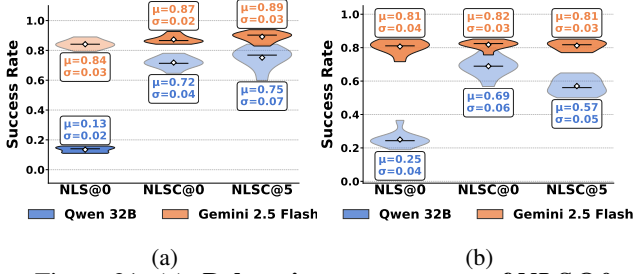


Figure 21: (a): Debugging success rates of NLS@0, NLSC@0, and NLSC@5 for Gemini-2.5 Flash and Qwen-2.5 32B Coder for buggy *combinational circuit* design codes. (b): Debugging success rates of NLS@0, NLSC@0, and NLSC@5 for Gemini-2.5 Flash and Qwen-2.5 32B Coder for buggy *sequential circuit* design codes.

shapes are top-heavy across all configurations. These upper sections indicate a ceiling effect – the model consistently averages a high score and hits the maximum possible success rate with very few outliers. In contrast, **DeepSeek R1** in the NLS@0 configuration shows a flat, stretched shape, meaning its performance is effectively random—sometimes good, often bad. Adding prompts (NLSC@0 and NLSC@5) compresses this shape into a tighter blob in the upper range, showing that structure improves the score and stabilizes the model’s behavior.

For sequential designs, we see that **Gemini-2.5 Pro** remains consistent; the violins are compact and narrow, showing little variation between different runs. The interesting detail appears in **DeepSeek R1**. In the NLS@0 setting, the mass is concentrated at the bottom (consistent failure). While the NLSC@0 prompt moves this mass clearly upward, the NLSC@5 (few-shot) configuration results in a wider, fatter shape. This visible expansion in width indicates that while few-shot examples help some test cases, they introduce higher variance in others, making the model less predictable than with simple instructions.

The visual spread observed in this experiment shows that DeepSeek R1’s results distributions suggests that the model gets “noisy” when given few-shot examples for complex state logic. In contracts, Gemini-2.5 Pro scales cleanly with more data at its disposal.

C.2.2 Gemini-2.5 Flash and Qwen-2.5 Coder

We extend our analysis to **Gemini-2.5 Flash** and **Qwen-2.5 Coder** using violin plots to visualize their stability and responsiveness to

different prompting strategies. Considering the combinational circuits, Figure 21a reveals a contrast in baseline capability. **Gemini-2.5 Flash** is remarkably consistent; even in the simple NLS@0 configuration, the distribution is concentrated high up ($\mu = 0.84$), and adding context in NLSC@ 5 only slightly tightens this top-heavy shape ($\mu = 0.89$). It works well “out of the box.” In contrast, **Qwen-2.5 Coder** is effectively broken in the NLS@0 setting, with a flat distribution stuck at the bottom ($\mu = 0.13$). However, the violin shape changes dramatically with the NLSC@0 prompt, jumping massively to a median of $\mu = 0.72$. This “gap” proves that Qwen possesses the logic to solve these circuits but is completely dependent on specific instructions to unlock it, whereas Gemini-2.5 Flash is self-sufficient.

For sequential designs, Figure 21b highlights a critical weakness in Qwen’s handling of context. **Gemini-2.5 Flash** remains “prompt-invariant”; its violins are almost identical across all three settings ($\mu \approx 0.81$), showing that neither instructions nor few-shot examples significantly change its stable behavior. **Qwen-2.5 Coder**, however, shows a unique regression. While it improves from NLS@0 ($\mu = 0.25$) to NLSC@0 ($\mu = 0.69$), adding the few-shot examples in NLSC@5 actually hurts performance, dropping the median to $\mu = 0.57$. The violin shape for NLSC becomes wider and shifts lower than NLS, indicating that for this model, the extra text from the few-shot examples acts as a distraction rather than a guide.

The violin plots observed in this experiment expose a “Contextual Distraction” effect in Qwen-2.5 Coder. While Gemini-2.5 Flash ignores the prompt format and relies on its internal reasoning (staying flat around $\mu = 0.81$), Qwen is highly sensitive. Crucially, in sequential tasks, “more is less” – simple instructions (NLSC@0) work best, while the longer context of few-shot learning (NLSC@5) confuses the model, causing a performance drop of 12%. This suggests smaller open-source models may struggle to attend to relevant details when the prompt becomes too long. This comparison highlights a trade-off. Gemini-2.5 Flash is robust, de-

livering consistent high scores regardless of the prompt method. In contrast, Qwen-2.5 Coder is more sensitive: it fails without instructions (NLS@0) and becomes better with NLSC@0 and NLSC@5.